https://dx.doi.org/10.22161/ijaers.6.4.4 ISSN: 2349-6495(P) | 2456-1908(O)

# Optimization of metakaolin-based Geopolymer Composite using Sisal Fibers, response Surface Methodology, and Canonical Analysis

Lorayne Cristina Silva, Rondinele Alberto dos Reis Ferreira, Leila Aparecida de Castro Motta, Lucas Bellini Machado

Civil Engineering School, Federal University of Uberlândia, 38400-902, Uberlândia, MG, Brazil

***Abstract*—*In the present context, geopolymer appears as an ecologically viable alternative compared to Portland cement, due to lower $CO_2$ emissions rate. The objective of this work is to study reinforced geopolymer pastes with elongated sisal fibers by means of parameters such as flexural strength. For this, metakaolinwas used as an aluminosilicate source material in addition to a combination of sodium silicate and sodium hydroxide as the activator solution. The influence of the independent variables sisal fiber percentage, molar ratio between activator and metakaolin, and the curing time was evaluated through an experimental design. The statistical model of central composite planning was used to optimize the results obtained. The best value for the modulus of rupture was of approximately 9.3 MPa, obtained with 2 days curing, with the activator/metakaolin ratio of 0.59 and percentage of sisal fiber de 4.34.***

***Keywords*—*Mechanical properties, Modulus rupture, Natural fibers, Sisal fibers.***

## I. INTRODUCTION

Among the challenges of the construction materials industry is the creation of new technologies that include reducing the emission of carbon dioxide ($CO_2$) and other pollutants, recycling of industrial waste and by-products, improving the performance of materials, in order to meet more ambitious design demands and higher durability requirements [1,2].

Alkaline activation of the geopolymer has been emphasize due to the potential of reduction of carbon dioxide emissions compared to materials based on Portland cement [1], being possible a reduction of up to 64% in greenhouse gas emissions [3]. The term geopolymeris used to describe alkali-activated low calcium aluminosilicate binders. This definition covers the use of pozzolans and blast furnace slag as precursor materials, but Portland cement may still be added in minor amounts [4]. In addition, properties such as excellent mechanical strength5, durability for acid attack6 and high fire resistance [7,8], make this material economically suitable for use in infrastructure employments. It should be noted, however, that the manufacturing process of this material usually requires high cure temperature and pH, which may compromise its field use, being important the development of a system with ambient temperature cure [9].

The process of hardening of the geopolymer occurs through the activation of a solid in an alkaline system [10], being frequently used as alkaline liquid combinations of sodium hydroxide (NaOH) or potassium hydroxide (KOH) with sodium or potassium silicate. According to [11], the solutions of activation of sodium silicate and sodium hydroxide increase the polymerization process of the ionic species present in the system. However, is essential that this combination between the two activators is balanced to maintain the high pH of the system and a high content of soluble silicon ions ($Si^{4+}$).

[5,12] affirm that there is potential for the application of geopolymer concretes in the prefabricated industry due to the greater control of handling and curing of the materials in these places, besides the capacity of use of the geopolymer in reinforced composites with fibers, prefabricated slabs for paving, bricks and prefabricated pipes. According to [13], in 2007 the Australian company Zeobond commercially launched, on a pilot scale, a geopolymeric concrete, called E-CreteTM, whose base material is a mixture of fly ash and blast furnace slag. Their applications range from infrastructure works to licensed repairs.

There are still challenges that geopolymers have to be adopted in the construction industry. According to [5,14] among them: different nomenclatures used in the literature to define geopolymeric material, high cost and risk management of the alkaline solution, misconceptions about geopolymeric properties, mainly from the cement industry, which affirms that alkali is detrimental to all systems. In addition, the adoption of composition-based construction standards, where a maximum amount of

*https://dx.doi.org/10.22161/ijaers.6.4.4* *ISSN: 2349-6495(P) | 2456-1908(O)*

additional cementitious material is allowed. It is also observed the difficulty in practicing steam cures or high temperatures required for certain geopolymers, with a conservative stance of the construction industry in which it refers to new products.

Moreover, the geopolymer, as well as Portland cement-based materials, have fragile type rupture mode [15]. An alternative to improve the mechanical properties is the incorporation of fibers in the matrix, which promote an increase of the toughness and improvement of the resistance to the flexion through the control of propagation of the fissures [16]. In this context, the use of natural fibers as reinforcement material is notable, since, compared to synthetic fibers, they have low preparation energy, what can justify the lowest cost [17]. Several natural fibers have already been used in geopolymers to improve mechanical performance, such as cotton [18], flax [19], Luffacylindrical [20] and bamboo fibers [21].

Regarding the shape and distribution of the fibers, two types of fiber reinforcement commonly used are mentioned, the continuous one, characterized by long fibers and incorporation through blankets or layers, and the short and discrete fibers, whose length is less than 50 mm and are introduced into the matrix by means of mixing or spraying techniques. In the configuration of continuous fibers, they can be aligned in a preferential direction, unlike the conformation assumed by the short and discrete ones, in which the fibers assume random orientation [22].

The effect of each parameter as well as of their interactions on modulus of rupture was studied using a central composite design (CCD) coupled with response surface method (RSM) and optimized by canonical analysis technique. The CCD consists in a first order factorial design ($2^k$) with additional points (center points and axial points). The central composite design (CCD) together with the response surface methodology (RSM) permit to find the optimum operating conditions with a reduced number of experiments [23] by estimating the main effects of each variable linear, quadratic and the interaction between the variables [24,25]. RSM enables to identify new operating conditions that produce desired improvements. According to [26], optimal operating conditions can be obtained by combining the adjusted response surface methodology with canonical analysis that is the reduction of the response surface that allows determining the nature of the stationary point and the response system.

Considering the heterogeneity of methodologies and results presented in the literature, the objective of this work was to analyze the influence of the variables sisal fiber percentage, the mass ratio between activator and metakaolin mass and curing time in the production and characterization of geopolymer composites.

## II. MATERIALS AND METHODS

### 2.1 Characteristics of materials

#### 2.1.1 Sisal fibers, metakaolin, sodium hydroxide and sodium silicate

The sisal fiber was acquired by SisalsulIndústria e ComércioLtda located in the city of São Paulo – Brazil. The metakaolin used in this investigation was donated by Metacaulim do BrasilIndústria e ComércioLtda, located in the city of Jundiaí, state of São Paulo - Brazil. A combination of sodium hydroxide (NaOH) and sodium silicate ($Na_2SiO_3$) was used as alkaline solution for the dissolution of aluminosilicate phases. Sodium hydroxide was present in micro pearl form and was acquire by Dinâmica Química Contemporânea Ltda. The sodium silicate, purchased by Una-Prosil, have oxides ratio equals 2.0 ($SiO_2/Na_2O$). The fibers were submitted to tensile test at speed application equals to 0.4 mm/min until material rupture in an INSTRON model 5982 with 5 kN load cell.

### 2.2 Materials characterization

#### 2.2.1 X-ray diffraction analysis (XRD) of the metakaolin and geopolymer

The RIGAKU, Miniflex model, with CuKα radiation (1.540 Å) was used to identify the characteristics peaks presented in 2θ angle between 5° and 90° at a 0.02° step. The crystallographic datasets of the crystallographic database ICSD (Inorganic Crystal Structure Database) were used to analyse the obtained diffractograms. This study was carried out at the Multiuser Laboratory of the Institute of Chemistry of the Federal University of Uberlândia (IQ/UFU). The geopolymer were transformed into powder for characterization and later were sifted in a sieve with 75 μm opening.

### 2.3 Design of experiments (DOE)

The central composite design was chosen as the experimental design for the development of the analytical procedures, with the input variables *x1, x2, ... xn* scaled to coded levels [27], which ranged from (-α), corresponding to the minimum level, and (+α) equivalent to the maximum level, with an alpha of orthogonality (α) of 1.41421. Table 1 show the coded and decoded values of the variables, determined by equations 1, 2 and 3.

*https://dx.doi.org/10.22161/ijaers.6.4.4* *ISSN: 2349-6495(P) | 2456-1908(O)*

*Table.1: Coded and uncoded levels of variables used for central composite design.*

| Parameters | Symbol | | Codedlevels | | | | |
|---|---|---|---|---|---|---|---|
| | Uncoded | Coded | -1.414 | -1 | 0 | 1 | 1.414 |
| Sisal fibers (wt%) | %sisal | $x_1$ | 0 | 0.85 | 3 | 5.15 | 6 |
| Activator/metakaolinratio | NaSi/Met | $x_2$ | 0.352 | 0.41 | 0.55 | 0.69 | 0.748 |
| Cure time (days) | C.T. | $x_3$ | 1 | 5 | 14.5 | 24 | 28 |

$$x_1 = \frac{(\%sisal - 3.0)}{2.15} \quad (1)$$

$$x_2 = \frac{(NaSi/Met - 0.55)}{0.14} \quad (2)$$

$$x_3 = \frac{(C.T. - 14.5)}{9.5} \quad (3)$$

Where %sisal, NaSi/Met and C.T. are the variables percentage of sisal in the geopolymer, sum of the masses of sodium (Na) and silicate (Si) by the mass of metakaolin, and cure time, respectively.

The overall analyses of the experimental data was performed using the software *Statistica12*, and the experimental data were submitted to a multiple regression with the purpose of measuring the effects of the studied variables for later adjustment of the model. The significance level of 10% was adopted for the analysis of the regression parameters [24].

2.3.1 Optimization

According to [26], optimal operating conditions can be obtained by combining the adjusted response surface methodology with canonical analysis. The optimization ofthe operating conditions for the modulus of rupture was performed using the canonical analysis technique. The response function can be expressed in terms of the parameters, according to Equation (4):

$$\hat{y} = b_0 + \underline{x}'\underline{b} + \underline{x}'B\underline{x} \quad (4)$$

where,

$$\underline{x}' = \begin{bmatrix} x1 \\ x2 \\ \vdots \\ xk \end{bmatrix}; \ \underline{b} = \begin{bmatrix} b1 \\ b2 \\ \vdots \\ bk \end{bmatrix}; \ \underline{B} = \begin{bmatrix} b11 & \frac{b12}{2} & \dots & \frac{b1k}{2} \\ \frac{b21}{2} & b22 & \dots & \frac{b2k}{2} \\ & \vdots & & \\ \frac{bk1}{2} & \frac{bk2}{2} & \dots & bkk \end{bmatrix}$$

The optimal condition (global maximum point, global minimum or saddle point) is obtained through the derivative of the adjusted surface equation in relation to the vector of variables, this value corresponding to zero in the case of the stationary point, as presented in Equations 5 and 6.

$$\frac{\partial \hat{y}}{\partial \underline{x}} = \frac{\partial}{\partial \underline{x}}\left[\hat{y} = b_0 + \underline{x}'\underline{b} + \underline{x}'B\underline{x}\right] = \underline{b} + B\underline{x} = \underline{0} \quad (5)$$

$$x_0 = -1/2B^{-1}b \quad (6)$$

The nature of the stationary point is defined by the translation the adjusted surface from the origin (*x1, x2, x3, ...xk*) = (0,0,0, ... 0) to the stationary point $\underline{x}^0$, (*w1, w2, w3, ..., wk*), whose axes correspond to the main ones of the contour system, represented by Equation 7:

$$\hat{y} = \hat{y}_0 + \lambda_1 w_1^2 + \lambda_2 w_2^2 + \ldots + \lambda_k w_k^2 \quad (7)$$

Where $\hat{y}$ is estimated response at stationary point and $\lambda_1$are thecharacteristics roots of the equation.

The determination of the nature of the stationary point $\underline{x}_0$ is analyzed by the characteristic root signals, where$\lambda_i < 0$, is the maximum response point, $\lambda_i > 0$, minimum response point and $\lambda_i$ for different signals, saddle point. The canonical analysis was implemented using the software *Maple17*.

2.4 Geopolymer preparation

The fibers were moistened and aligned on a sheet of filter paper. The fibers were weighed and cut into the size of the specimens (0.17 m length x 0.04 m wide), with more than one layer being added as necessary. The extremity was then secured with adhesive tape. The thickness of each specimen was 0.01 m. After making the fibers, the alkaline activators were then weighed and dissolved in distilled water, separately. The mass ratio of sodium silicate to sodium hydroxide was equal to 2.5 and the water-metakaolin ratio was 0.7. The molarity values of the sodium hydroxide and sodium silicate were 15 and 12 M, respectively, chosen according to reports in the literature. The NaOH solution was first mixed for 1 min with the $Na_2SiO_3$ solution and the extra water (corresponding to the water mass according to the water-metakaolin ratio). The mixture was then added to the metakaolin and homogenized for 5 min. Subsequently, a layer of the material was placed in the silicone forms, for subsequent addition of the blankets. Finishing occurred with another layer of geopolymer, with sealing of samples with plastic film and curing at room temperature (25 ± 5

*https://dx.doi.org/10.22161/ijaers.6.4.4* *ISSN: 2349-6495(P) | 2456-1908(O)*

°C). For each CCD formulation, five specimens were molded.

2.5 Composites characterization

2.5.1 Flexural strength test

The rupture test was performed under laboratory ambient conditions (25 ± 5 °C) between 1 and 28 days of age, obtaining the values of modulus of rupture. The rupture test method used was the four-point flexural test recommended by [28], in which the load application is done in two points of the sample, generating a constant moment between the points of load, using a Universal Machine of Instron brand tests, model 5982, and load cell of 5 kN. The distance between the lower supports was 150 mm and the load application speed was 2 mm/min.

2.5.2 Scanning electron microscopy (SEM) of the geopolymer

The ruptured specimens were cut using a circular saw, and they were impregnated with an epoxy resin and posteriorly sanded. Subsequently, the test specimens metallization was performed with gold in the Multiuser Laboratory of the Institute of Chemistry of the Federal University of Uberlândia (IQ/UFU) and the Dispersive Energy Spectroscopy (EDS) coupled to the MEV (model Vega3 and Tescan brand), was used to verify the composition of the matrix.

## III. RESULTS AND DISCUSSION

3.1 Characteristics of materials

3.1.1 Sisal fibers, metakaolin, sodium hydroxide and sodium silicate

The sisal fiber presented specific density of 1511 kg/m$^3$, with a diameter of230.14 µm (± 43.48). Young's modulus, elongation and strength were 11.47 GPa(± 2.78), 0.59 mm (± 0.09), and 371.61 MPa (± 81.63), respectively [29,30]. According to [17], the great variability of the results of tensile strength and modulus of elasticity can be explained by three factors: the parameters of the tests, the characteristics of the plants and the measurements of the sections fibers. The accuracy of the instrumentation, the length of the meter and the type of claw are some test conditions that may interfere in the final values of the mechanical properties of the fibers. Adding to this, as a characteristic of plants, one has the diversity of plant sources, ages, and types of processing and microstructure. Finally, the uncertainties in the measurement of the cross-sectional area of the fiber may lead to a discrepancy in the mechanical parameters. The metakaolin presented a particle diameter of 12 micrometer and a specific density of 2650 kg/m$^3$. According to with the chemical characterization, it presents expressive percentages of $SiO_2$ (51.57%) and $Al_2O_3$ (40.5%), making approximately 92% of these two compounds. It also has small amounts of $Fe_2O_3$ (2.8%), $Na_2O$ and $K_2O$ (< 1%) [31]. Sodium hydroxide has 98% purity and was dissolved in water to obtain a 15-molar solution. The sodium silicate, with a specific density of 570 kg/m$^3$, contains 52.1% of $SiO_2$ and 26.1% of $Na_2O$, with total solids equals 78.2%.

3.2 Materials characterization

3.2.1 X-ray diffraction analysis (XRD) of metakaolin

Fig. 1 shows the composition of metakaolin through the XRD pattern.

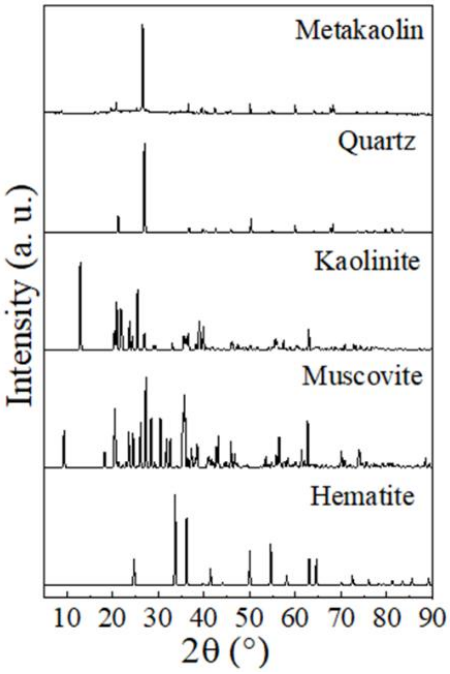


*Fig. 1.XRD patterns of the metakaolin.*

According to Fig. 1, observed a crystalline pattern, with no apparent halo, suggesting that amorphous phases are not present in large quantities. The main mineral phase was the quartz with 2θ diffraction peaks equal to 21.2º, 26.96º, 36.70º, 39.72º, 42.54º, 45.88º, 50.24º e 54.90º, 59.86º, 64.04º, 73.46º (ICSD-89281). In addition, kaolinite peaks evidenced, possibly, that calcination of kaolinite was not complete (2θ = 20.90º, 36.54º, 50.20º, 75.60º - ICSD - 68698). It was also observed the peak of impurities, such as muscovite (2θ = 36.42º, 45.90º, 54.80º, 60.04º - ICSD-60569) and hematite (2θ = 36.5º, 50.00º - ICSD - 15840) [32,33].

3.3 Design of experiments (DOE)

Table 2 shows the values of the response variable (modulus of rupture) for the 18 experiments of the experimental design obtained by the flexural tests.

https://dx.doi.org/10.22161/ijaers.6.4.4 ISSN: 2349-6495(P) | 2456-1908(O)

*Table 2.The experimental conditions studied in CCD matrix, with uncoded values of parameters.*

| E* | %sisal (%) | NaSi/Met | C.T. (days)** | M.R. (MPa)*** |
|---|---|---|---|---|
| 1 | 0.85 | 0.41 | 5 | 6.41 |
| 2 | 0.85 | 0.41 | 24 | 4.12 |
| 3 | 0.85 | 0.69 | 5 | 4.56 |
| 4 | 0.85 | 0.69 | 24 | 3.63 |
| 5 | 5.15 | 0.41 | 5 | 6.47 |
| 6 | 5.15 | 0.41 | 24 | 8.01 |
| 7 | 5.15 | 0.69 | 5 | 9.48 |
| 8 | 5.15 | 0.69 | 24 | 7.97 |
| 9 | 0.00 | 0.55 | 14.5 | 4.15 |
| 10 | 6.00 | 0.55 | 14.5 | 9.23 |
| 11 | 3.00 | 0.352 | 14.5 | 3.95 |
| 12 | 3.00 | 0.748 | 14.5 | 6.99 |
| 13 | 3.00 | 0.55 | 1.06 | 7.09 |
| 14 | 3.00 | 0.55 | 27.9 | 10.48 |
| 15 | 3.00 | 0.55 | 14.5 | 9.05 |
| 16 | 3.00 | 0.55 | 14.5 | 9.22 |
| 17 | 3.00 | 0.55 | 14.5 | 8.91 |
| 18 | 3.00 | 0.55 | 14.5 | 9.06 |

*E: Experimental plane; **Cure time; ***MR: Modulus of rupture

3.3.1 Modulus of rupture (M.R.)

A polynomial equation was developed that correlates the modulus of rupture (M.R.) in function of the independent variables, obtained by multiple regression, represented by equation 8.

$$M.R. = 8.97 + 1.7x_1 - 1.06x_1^2 + 0.41x_2 - 1.67x_2^2 + 0.13x_3 - -0.01x_3^2 + 0.66x_1x_2 + 0.41x_1x_3 - 0.21x_2x_3 \quad (8)$$

Where M.R. corresponding to Modulus of Rupture (MPa).

According to equation 8, the linear and quadratic variables of the percentage of sisal fiber ($x_1$) and the quadratic variable mass ratio between activator and metacaulim ($x_2$) were significant, representing the modulus of rupture at a 90% confidence level. Each parameter has a significance analysis according to the probability value (*p-value*). Significant variables had a *p-value* of less than 0.10 ($p < 0.10$). The coefficient of determination $R^2$, which is defined as the fraction of the total variance of the dependent variable that is explained by the model equation [34] obtained was 0.86. [35]recommend an $R^2$ value greater than 0.80 to obtain a good fit model. Since the presented variable has a higher than recommended value, it was possible to construct the response surfaces.

The percentage of sisal added in the matrix showed a positive effect (+1.70). However, when the addition of large amounts of sisal fibers occurs, the value of this parameter does not tend to increase the value of the response, which is probably due to the incorporation of residual air bubbles, from the process of filling the forms [18]. The same happened for the quadratic form of the variable that corresponds to the mass ratio between activator and metakaolin, in which larger quantities do not tend to increase the resistance value, possibly explained by the excess of unreacted material in the final compound, which, being leachate may interfere with the final resistance [36].

Fig. 2a shows the response surface for M.R. as function of the %sisal ($x_1$) and the NaSi/Met ratio ($x_2$), with C.T. at the central level ($x_3$ = 0). Observed that the highest values of mechanical resistance were reached when the %sisal ($x_1$) was at the upper limit of the studied range (+0.8) (corresponding to the decoded value of 4.72% of sisal fibers), and the NaSi/Met ($x_2$) ratio near the center point that is, with a decoded value of 0.55, obtaining a result of approximately 10 MPa. The amount of soluble silicon ions in the final compound, although important for increasing the rate of polymerization and formation of a denser structure [11,37], in excess may not react for gel formation, being leached and interfering with the ultimate strength of the geopolymer [38].

*https://dx.doi.org/10.22161/ijaers.6.4.4* *ISSN: 2349-6495(P) | 2456-1908(O)*

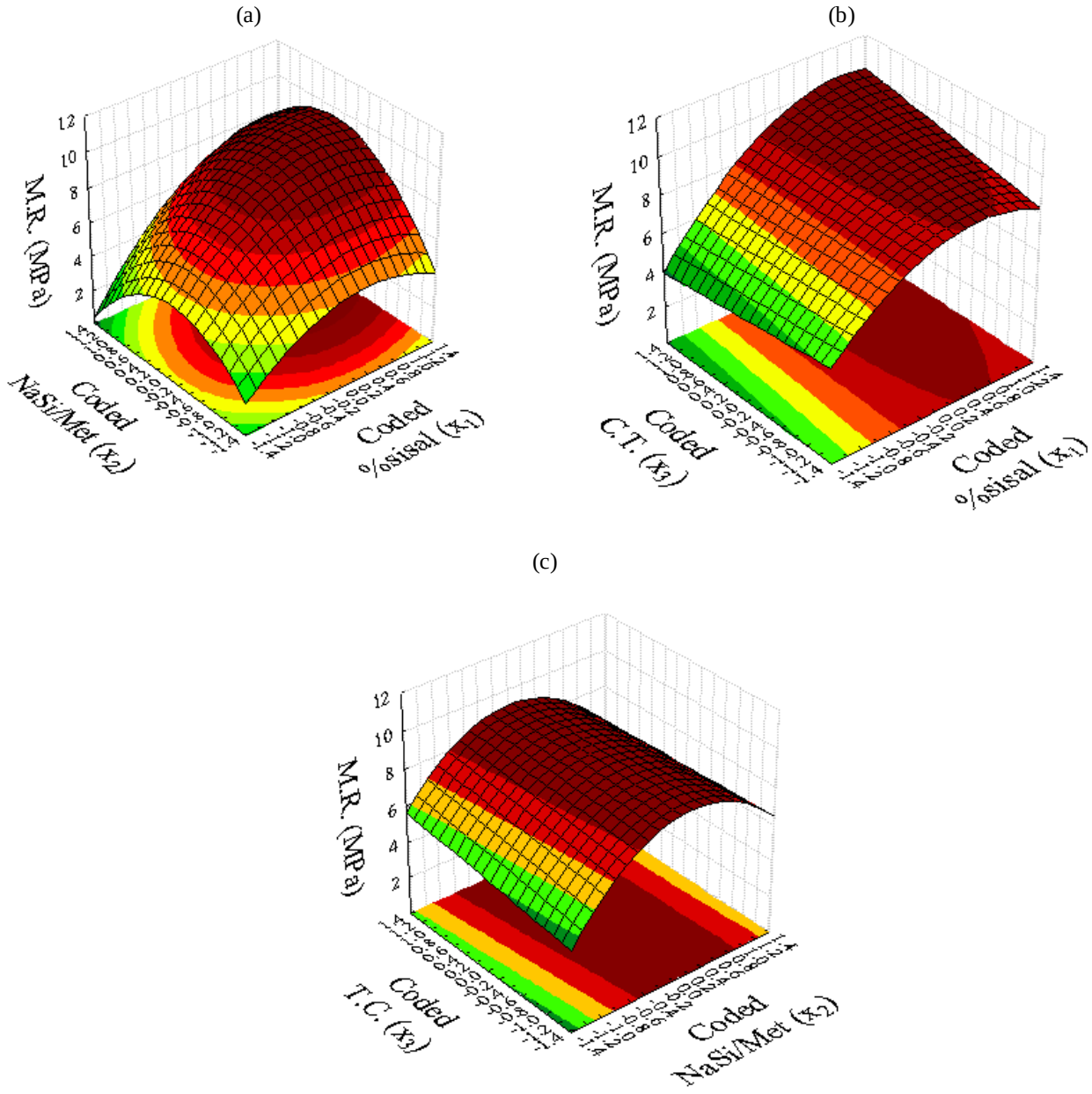


*Fig. 2. Response surface of the modulus of rupture: (a) C.T. at the central level (x3 = 0); (b) NaSi/Met the central level (x2 = 0); (c) %sisal at the central level (x1 = 0).*

Relative to the percentage of sisal in the final mixture, the amount of fibers has the tendency to increase the flexural strength controlling the propagation of cracks, which led the material to withstand a greater load[39].

Figure 2b shows the response surface for M.R. as function of %sisal ($x_1$) and C.T. ($x_3$), with NaSi/Met ratio at the central level ($x_2$ = 0). Observed the M.R. values increase with the %sisal ($x_1$) at a coded value of approximately +1.0 (5.15% sisal fibers as decoded value), with low C.T. ($x_3$), resulting in the M.R. value of approximately 10 MPa. As explained previously, the fiber, when inserted in the geopolymer matrix, acts as a stress transfer bridge through the cracks, generating a post-cracking load capacity. In addition, the geopolymerization process continues to occur for more advanced curing times and, as a result, the average strength increases [40].

Figure 2c shows the response surface for M.R. according to NaSi/Met ratio ($x_2$) and C.T. ($x_3$), with the %sisal at the central level ($x_1$ = 0). Observed an increase in the mechanical strength value for a NaSi/Met ratio ($x_2$) near the center point (decoded value of 0.55), with a low influence of C.T. ($x_3$). Thus, a value of about 9MPa was obtained. Silica is important for the continuous process of

*https://dx.doi.org/10.22161/ijaers.6.4.4* *ISSN: 2349-6495(P) | 2456-1908(O)*

geopolymerization and consequent improvement of the mechanical parameters. However, if mixed in excess, it tends to form unreacted grains, which negatively interfere with the strength of the final geopolymer.

3.3.2 Canonical analysis

Obtained the Equation 9 by reducing the quadratic form to the canonical form. According to the stationary point, it was verified the existence of a saddle point, that is, the characteristic roots ($\lambda_i$) have opposite signs and the stationary point is not characterized by a minimum or a maximum point (saddle point).

$$\hat{y} = +8.332 - 1.829w_1^2 - 0.931w_2^2 + 0.031w_3^2 \qquad (9)$$

Observed that, to optimize the rupture modulus that is, increase the value of this parameter, the variables $w_1$ and $w_2$ must be zero, since the response decreases in the direction of these, therefore, finding several values for$w_3$. From the presented variables, the following restrictions were applied, according to the equations 1, 2 and 3: $x_1 \geq -1.41421$, $x_2 \geq -3.928$, and $x_3 \geq -1.5263$, so that the values are physically possible.

Table 3 presents the decoded results, according to the recurrence equations, for the conditions in $x_1$, $x_2$ and $x_3$ and several values for $w_3$.

*Table 3. Values of $w_3$ according to the values decoded of $x_1$, $x_2$, $x_3$, and response prediction.*

| $w_3$ | 4.5 | 5.0 | 5.5 | 6.0 | 6.5 | 7.0 | 7.5 | 8.0 | 8.5 |
|---|---|---|---|---|---|---|---|---|---|
| %sisal | 3.968 | 4.156 | 4.345 | 4.534 | 4.723 | 4.912 | 5.101 | 5.290 | 5.490 |
| NaSi/Met | 0.601 | 0.599 | 0.597 | 0.595 | 0.593 | 0.591 | 0.589 | 0.587 | 0.586 |
| C.T. | -7.493 | -2.819 | 1.855 | 6.530 | 11.204 | 15.878 | 20.553 | 25.227 | 29.901 |
| M.R. | 8.965 | 9.114 | 9.277 | 9.457 | 9.652 | 9.863 | 10.090 | 10.332 | 10.589 |

According to Table 3, observed that, for values of $w_3 \leq$ 5.0, the value for curing time is physically impossible (-2.819). In addition, values of $w_3 \geq$ 8.5 were discarded as optimal points because presented a very small increase in resistance to curing times (C.T.) longer than 28 days. Thus, it was observed that the most adequate conditions for the optimization of the rupture modulus consisted of $w_3$ = 5.5, and $w_3$ = 6.0, with all values of the independent variables belonging to the studied range (Fig. 3).

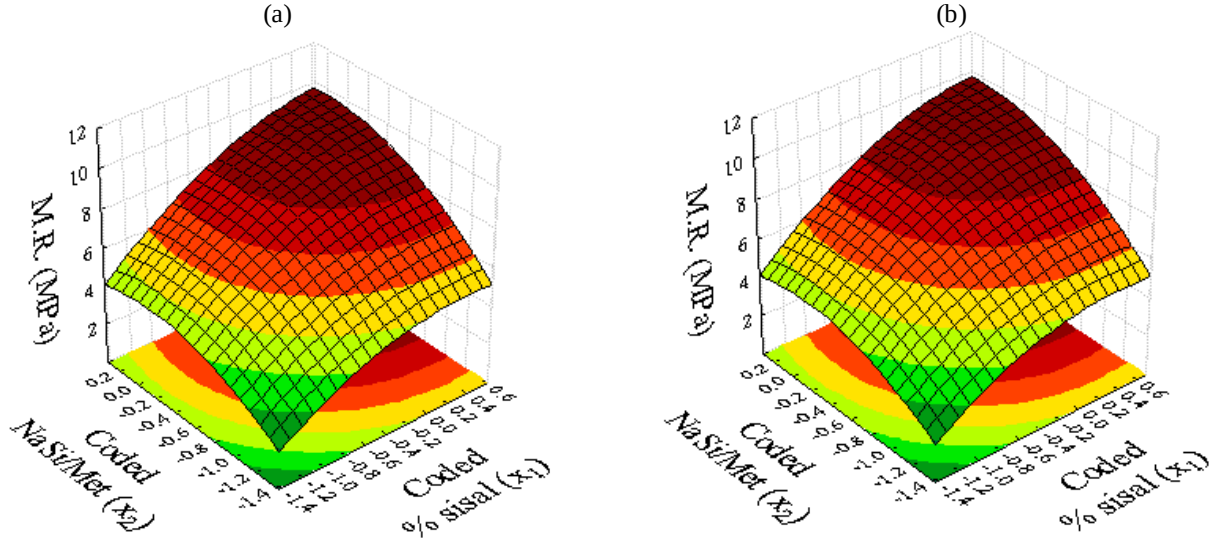


*Fig. 3. Optimized response surface: a) $w_3$ = 5.5; b) $w_3$ = 6.0.*

In addition, the values of $w_3$ = 5.5 and $w_3$ = 6.0 were chosen, once the curing time was the parameter that presented greater diversification of values when analyzed the results of modulus of rupture. Comparing $w_3$ = 5.5, and $w_3$ = 8, corresponding to approximate cure times of 2 and 25 days, respectively, observed that there was a very small increase in the M.R. value of approximately 11%.

*https://dx.doi.org/10.22161/ijaers.6.4.4* *ISSN: 2349-6495(P) | 2456-1908(O)*

This result indicated that the production of the geopolymer is feasible for lower cure times.

For the optimized conditions, $w_3$ = 5.5 and 6.0, values for the modulus of rupture of 9.27 and 9.45 MPa, respectively, were obtained. According to results presented in Table 2, a modulus of rupture of 9.22 MPawas obtained with 14.5 days of cure. With the optimization process, it was possible to obtain close values, working with times cure lower (approximately 2 days), reducing the geopolymer aging process by about 87%.

3.4 Geopolymer characterization

3.4.1 X-ray diffraction analysis (XRD)

Fig. 4 showsthe diffractograms of the geopolymers. Among the mineral phases identified, observed the quartz predominance, with 2θ diffraction peaks equal to 21.2º, 26.96º, 36.70º, 39.72º, 42.54º, 45.88º, 50.24º, 54.90º and 59.86º (ICSD-89281). Additionally, peaks present in the raw material remained in the geopolymer pattern, such as kaolinite (2θ = 20.90º, 36.54º, 50.20º, 75.60º - ICSD - 68698), muscovite (2θ = 36.42º, 45.90º, 54.80º, and 60.04º) and the hematite (2θ = 36.5º and 50º - ICSD - 15840)[41,42]. Observed that the crystallized structures present in the metakaolindiffractogram also appear in the final geopolymer compound, in smaller quantities, due to the possible hard dissolution, being these non-reactive crystals, which did not participate in the geopolymerization reactions, with a possible filling function [42,43,44]. [42] argued that secondary minerals such as quartz and muscovite play an important role in acidic resistance since the release of alkali cations in the solution is hampered, resulting in less degradation and loss of weight. In addition to the crystalline peaks of metakaolin, there was no new crystalline reaction product formed, as also observed by [45].

[46] explain that, for times shorter than 240 days, the binder does not have enough time to grow in a well-defined structure, thus presenting in amorphous and semi-crystalline phases. One of the possible explanations for the non-appearance of amorphous halos, characteristic of geopolymers would be the high quartz peak, which may make their presence less evident [44].

3.4.2 Scanning electron microscopy (SEM)

According to SEM analyses, observed a good matrix-fiber interaction in the experimental planes (E) studied. Since there was no total rupture of the test specimen, a fact also observed by [15], the analyzed section is presented in the sanded form, and it is not possible to verify the mechanism of rupture of the sisal fiber. The presence of fiber detachment in the matrix possibly occurred due to the drying process of the samples in an oven for further preparation for microscopic analysis. Analyses of the EDS on the fiber (represented by the rectangle) proved the presence of the matrix within the same (Fig. 5) where chemical elements belonging to the matrix (Si, Al, O, Na) and fiber (such as carbon, denoted by the letter C) were identified. Observed in the geopolymer of the experimental plane E2 (Fig. 6) that, despite the good matrix-fiber interaction, occurred of fiber agglomerations, which can result in poor interfacial adhesion and in the creation of pores in the matrix, contributing to the decrease of flexural strength of the composite [18].

The presence of pores and cracks of varying widths can be observed in practically all the samples. According to [47], the existence of pores in the matrix possibly was caused by the entrapment of bubbles resulting from the dissolution process and geopolymerization reaction.

Fig. 7 shows the EDS of the geopolymer of to the experimental plane 3. Analyses were performed on the darker color particles in the geopolymer and the result revealed that they are unreacted $SiO_2$ particles (represented by the rectangle). Noted that there is a large presence of this material distributed in the matrix, which possibly influenced the results obtained for mechanical strength of the composite since the unreacted material tends to be less resistant than the geopolymer [36,38].

The same phenomenon was observed for the experimental planes 3, 4, 5, 7, 8, 11, 12 and 13, 15, 16, 17 and 18. The experimental planes E3, E4, E7 and E8 are those with activator/metakaolin ratio equal to 0.69, and possibly the presence of unreacted material is due to the excess amount of silicon ions in the mixture, and even at 24 days of cure it is still possible to observe the existence of these materials. After 24 days of cure, it was still possible to observe the presence of these materials in the geopolymer. The same happened, probably, for the experimental plane 12, which presented an activator/metakaolin ratio of 0.748. The geopolymer for experiment 11 (E11), with a cure time of 14.5 days, presented the lowest activator/metakaolin ratio (NaSi/Met), resulting in one of the less dense matrices between the experimental planes. According to [37], a smaller amount of silicate present in the activator solution tends to decrease the rate of geopolymerization, resulting in a less dense and compact matrix at shorter times cure.

Fig. 8 shows the surface of the geopolymer of experimental plane 9 (E9). This geopolymer presented a different configuration compared to the other samples since it was not reinforced with sisal fibers. Observed in this geopolymer that the rupture occurred in a fragile way, as was also observed by [15,43]. Probably because it was not subjected to the sanding process of the sample, the surface presented a rough surface, with homogeneous and

*https://dx.doi.org/10.22161/ijaers.6.4.4* *ISSN: 2349-6495(P) | 2456-1908(O)*

compact structures, with the presence of pores that, as previously stated, may have been incorporated in the binder dissolution process or of the geopolymerization reactions [47].

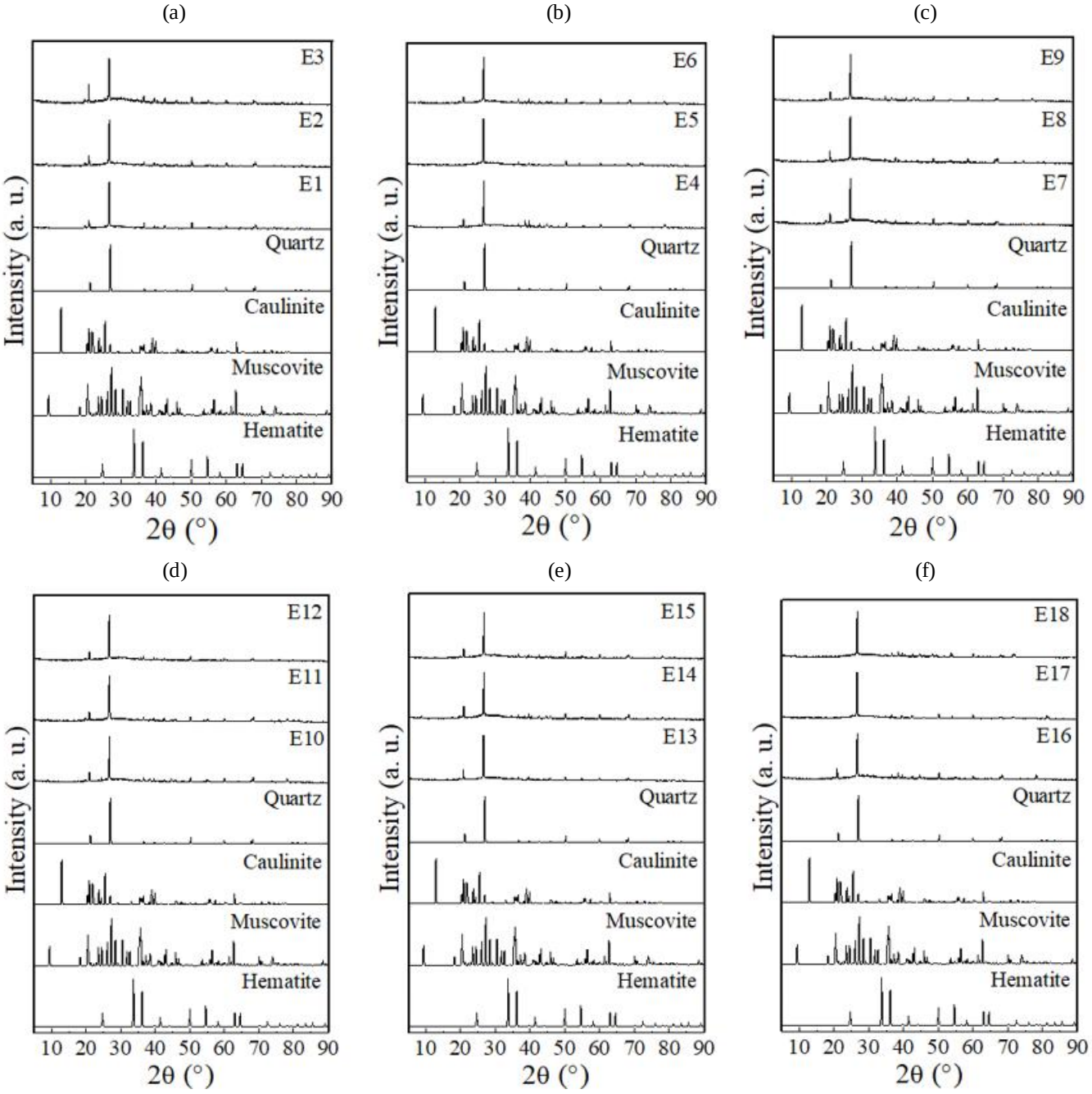


*Fig. 4. XRD patterns of the geopolymers: a) E1, E2, E3; b) E4, E5, E6;c) E7, E8, E9; d) E10, E11, E12,* e) E13, E14, E15; f) E16, E17, E18.

*https://dx.doi.org/10.22161/ijaers.6.4.4* *ISSN: 2349-6495(P) | 2456-1908(O)*

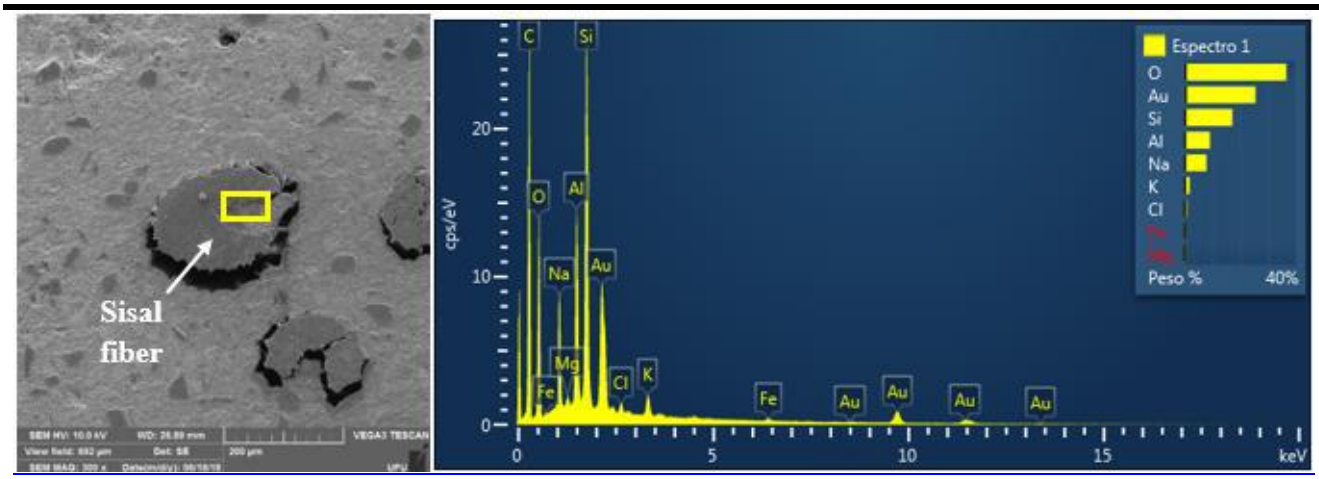


*Fig. 5. EDS for matrix impregnated on sisal fiber.*

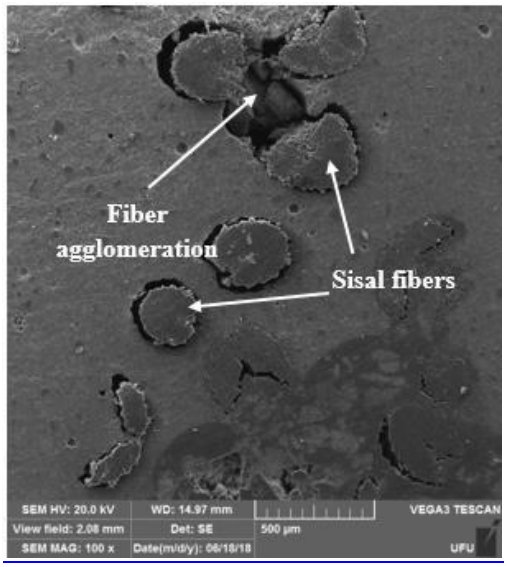


*Fig. 6.Fiber agglomeration in the geopolymer of experimental plane 2 (E2).*

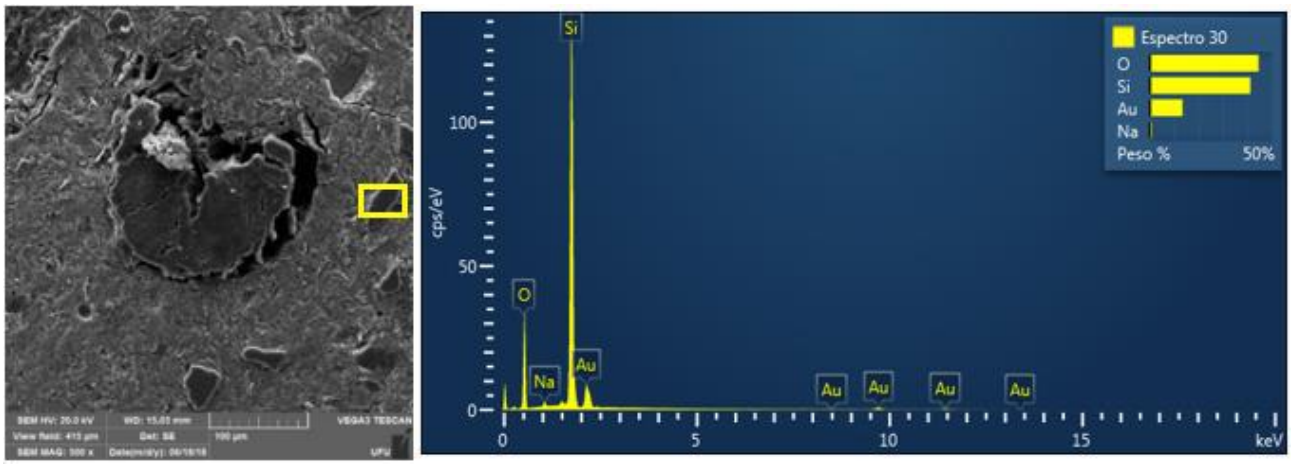


*Fig. 7. EDS of the dark particles present in the geopolymer of experimental plane 3 (E3).*

*https://dx.doi.org/10.22161/ijaers.6.4.4* *ISSN: 2349-6495(P) | 2456-1908(O)*

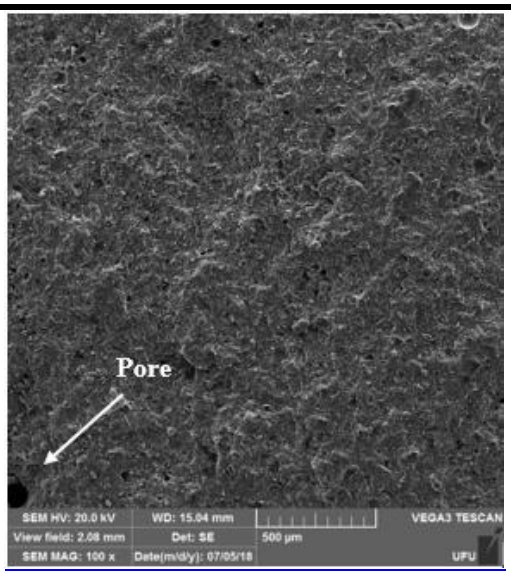


*Fig.8: Surface of the geopolymer of experimental plane 9 (E9).*

## IV. CONCLUSION

The use of long sisal fibers improved the mechanical properties of the composites, increasing the modulus of rupture compared to the non-reinforced matrix. Unreacted products were found in the matrices with higher amount of activator and/or shorter curing times, demonstrating that may influence in the final mechanical strength value. The best value for the modulus of rupture was of approximately 9.3 MPa, obtained with 2 days curing, with the activator/metakaolin ratio of 0.59 and percentage of sisal fiber de 4.34, evidencing the potential of the geopolymer with the use of fibers and high initial strength.

## ACKNOWLEDGEMENTS

The authors would like to acknowledge CNPq, CAPES and FAPEMIG for supporting this work and Metacaulim do BrasilIndústria e ComércioLtda for the metakaolin donation.

## REFERENCES

[1] Mikulcic, H., Cabezas, H., Vujanovic, M., Duic, N. (2016). Environmental assessment of different cementmanufacturing processes based on Energy and Ecological Footprint analysis. Journal of Cleaner Production, 130, 213-221.

[2] Provis, J.L. (2014). Geopolymers and other alkali activated materials: why, how, and what? Materials and Structures, 47, 11-25.

[3] McLellan, B.C., Williams, R.P., Lay, J., Van Riessen, A., Corder, G.D. (2011). Costs and carbon emissions for geopolymer pastes in comparison to ordinary portland cement. Journal of Cleaner Production, 19, 1080-1090.

[4] Provis, J.L. (2017). Alkali-activated materials. Cement and Concrete Research, 114, 40-48.

[5] Aleem, M.I., Arumairaj, P.D. (2012).Geopolymer concrete – A review. IJSET, 1,118-122.

[6] Aldred, J.M. (2013). Engineering properties of a proprietary premixed geopolymer concrete. In: Proceedings Concrete Institute of Australia Biennial Conference in Concrete.

[7] Zhao, R., Sanjayan, J.G.C. (2011). Geopolymer and Portland cement concretes in simulates fire. Magazine of Concrete Research, 63, 163-173.

[8] Rangan, B.V. (2014). Geopolymer concrete for environmental protection. The Indian Concrete Journal, 88 (41-48), 50-59.

[9] Singh, B., Ishwarya, G., Gupta, M., Bhattacharyya, S.K. (2015).Geopolymer concrete: a review of some recent developments. Construction and Building Materials, 85, 78-90.

[10] Schneider, M., Romer, M., Tschudin, M., Bolio, H. (2011). Sustainable cement production—present and future. Cement and Concrete Research, 41 (7), 642-650.

[11] Fernández-Jiménez, A., Palomo, A. (2005).Composition and microstructure of alkali activated fly ash binder: Effect of the activator. Cement and Concrete Research, 35, 1984-1992.

[12] Roy, D.M. (1999). Alkali activated cements – Opportunities and challenges. Cement and Concrete Research, 29, 249-254.

[13] Van Deventer, J.S.J, Provis, J.L., Duxson, P. (2012). Technical and commercial progress in the adoption of geopolymer cement. Minerals Engineering, 29, 89-104.

[14] Duxson, P., Provis, J.L., Lukey, G.C., Van Deventer, J.S.J. (2007). The role of inorganic polymer

*https://dx.doi.org/10.22161/ijaers.6.4.4* *ISSN: 2349-6495(P) | 2456-1908(O)*

technology in the development of green concrete. Cement and Concrete Research, 37 (12), 1590-1597.

[15] Lin, T., Jia, D., He, P., Wang, M., Liang, D. (2008). Effects of fiber length on mechanical properties and fracture behavior of short carbon fiber reinforced geopolymer matrix composites. Materials Science and Engineering: A,497, 181-185.

[16] Silva, F.A., Mobasher, B., Toledo Filho, R.D. (2009). Cracking mechanisms in durable sisal fiber reinforced cement composites. Cement and Concrete Research, 31, 721-730.

[17] Silva, F.A., Chawla, N., Toledo Filho, R.D. (2010). Mechanical behavior of natural sisal fibers. Journal of Biobased Materials and Bioenergy, 24, 777-785.

[18] Alomayri, T., Shaikh, F.U.A., Low, I.M. (2013). Characterisation of cotton fibre-reinforced geopolymer composites. Composites Part B: Engineering, 50, 1-6.

[19] Alzeer, M., Mackenzie, K. (2013). Synthesis and mechanical properties of novel composite of inorganic polymers (geopolymers) with unidirectional natural flax fibres (*phormiumtenax*). Applied Clay Science, 75-76, 148-152.

[20] Alshaaer, M., Mallouh, S.A., Kafawein, J., Fahmy, T., Kallel, A., Rocha, F. (2017). Fabrication, microstructural and mechanical characterization of Luffa Cylindrical Fibre - Reinforced geopolymer composite.Applied Clay Science, 143, 125-133.

[21] Sankar, K., Ribeiro, R.A.S., Ribeiro, M.G.S., Kriven, W.M. (2017). Potassium - Based Geopolymer Composites Reinforced with Chopped Bamboo Fibers. Journal of the American Ceramic Society, 100, 49-55.

[22] Bentur A., Mindess S. second eds. Fibre reinforced cementitious composites. Grã-Bretanha; 2007.

[23] Bouaid, A., Martinez, M., Aracil, J. (2007). A comparative study of the production of ethyl esters from vegetable oils as a biodiesel fuel optimization by factorial design. Chemical Engineering Journal, 134, 93-99.

[24] Santana, R.C., Santos, M.A., Ataíde, C.H., Barrozo, M.A.S. (2010). Evaluation of the influence of process variables on flotation of phosphate. Materials Science Forum, 660-661, 555-560.

[25] Bezerra, M.A., Santelli, R.E., Oliveira, E.P., Villar, L.S., Escaleira, L.A. (2008). Response surface methodology (RSM) as a tool for optimization in analytical chemistry. Talanta, 76, 965-977.

[26] Santana, R.C., Farnese, A.C.C., Fortes, M.C.B., Ataíde, C.H., Barrozo, M.A.S. (2008).Influence of particle size and reagent dosage on the performance of apatite flotation. Separation and Purification Technology, 64, 8-15.

[27] Khayet, M., Cojocaru, C., Essalhi, M. (2011). Artificial neural network modeling and response surface methodology of desalination by reverse osmosis. Journal of Membrane Science, 368, 202-214.

[28] RILEM. Technical Committee 49 TRF. (1989). Test for determination of modulus of rupture and limit of proporcionality of thin fibre reinforced cement section – Matériauxet Constructions, 17, 441-443.

[29] Munawar, S.S., Umemura, K., Kawai, S. (2007).Characterization of the morphological, physical, and mechanical properties of seven nonwood plant fiber bundles. Journal of Wood Science, 53, 108-113.

[30] Silva, F.A., Toledo Filho, R.D., Melo Filho, J.A., Fairbairn, E.M.R. (2011). Physical and mechanical properties of durable sisal fiber-cement composites. ConstructionandBuildingMaterials, 10, 2022-2027.

[31] Rabello, M. (2003). Estudo da influência do MetacaulimHP como adição de alta eficiência em concretos de cimento Portland. Escola Politécnica da Universidade de São Paulo, 1-65.

[32] Paiva, H., Velosa, A., Cachim, P., Ferreira, V.M. (2016). Effect of pozzolans with different physical and chemical characteristics on concrete properties. Materiales de Construcción, 66, 1-12.

[33] Wan, Q., Rao, F., Song, S., Gárcia, R.E., Estrella, R.M., Patino, C.L., Zhang, Y. (2017). Geopolymerization reaction, microstructure and simulation of metakaolin-based geopolymers at extended Si/Al ratios. Cement and Concrete Composites, 79, 45-52.

[34] El-Khaiary, M., Malash, G. (2011). Common data analysis errors in batch adsorption studies. Hydrometallurgy, 105, 314-320.

[35] Jamil, N.H., Halim, N.R.A., Sarbon, N.M. (2013). Optimization of enzymatic hydrolysis condition and functional properties of eel (*Monopterus* sp.) protein using response surface methodology. Food Research International, 23, 1-9.

[36] Gao, K., Lin, K.L., Wang, D., Hwang, C.L., Tuan, B.L.A., Shiu, H.S., Cheng, T.W. (2013). Effect of nano-$SiO_2$ on the alkali-activated characteristics of metakaolin-based geopolymers. Construction and Building Materials, 48, 441-447.

[37] Moon, J., Bae, S., Celik, K., Yoon, S., Kim, K.H., Kim, K.S., Monteiro, P.J.M. (2014). Characterisation of natural pozzolan-based geopolymeric binders. Cement and Concrete Composites, 53, 97-104.

[38] Duxson, P., Provis, J.L., Lukey, G.C., Mallicoat, S.W., Kriven, W.M., Van Deventer, J.S.J. (2005). Understanding the relationship between geopolymer composition, microstructure and mechanical

*https://dx.doi.org/10.22161/ijaers.6.4.4* *ISSN: 2349-6495(P) | 2456-1908(O)*

properties. Colloids and Surfaces A: Physicochemical and Engineering Aspects, 269, 47-58.

[39] Nguyen, H., Carvelli, V., Adesanya, E., Kinnunen, P., Illikainen, M. (2018). High performance cementitious composites from alkali-activated ladle slag reinforced with polypropylene fibers. Cement and Concrete Composites, 90, 150-160.

[40] Palomo, A., Grutzeck, M.W., Blanco, M.T. (1999). Alkali-activated fly ashes – A cement for the future.Cement and Concrete Research, 29, 1323-1329.

[41] Zhang, Z., Wang, H., Provis, J.P., Bullen, F., Reid, A., Zhu, Y. (2012). Quantitative kinetic and structural analysis of geopolymers. Part 1. The activation of metakaolin with sodium hydroxide. Thermochim. Acta, 539, 23-33.

[42] Bouguermouh, K., Bouzidi, N., Mahtout, L., Pérez-Villarejo, L., Martínez-Cartas, M.L. (2017). Effect of acid attack on microstructure and composition of metakaolin-based geopolymers: The role of alkaline activator. Journal of Non-Crystalline Solids, 463, 128-137.

[43] He, J., Zhang, J., Yu, Y., Zhang, G. (2012). The strength and microstructure of two geopolymers derived from metakaolin and red mud-fly ash admixtures: A comparative study. Construction and Building Materials, 30, 80-91.

[44] Zhang, M., El-Korchi, T., Zhang, G., Liang, J., Tao, M. (2014). Synthesis factors affecting mechanical properties, microstructure, and chemical composition of red mud–fly ash based geopolymers. Fuel, 134, 315-325.

[45] Yang, T., Zhu, H., Zhang, Z. (2017). Influence of fly ash on the pore structure and shrinkage characteristics of metakaolin-based geopolymer pastes and mortars. Construction and Building Materials, 153, 284-293.

[46] Zhang, Y.J., Wang, Y.C., Xu, D.L., Li, S. (2010). Mechanical performance and hydration mechanism of geopolymer composite refinforced by resin.Materials Science and Engineering: A, 527, 6574-6580.

[47] Tchakaouté, H.K., Ruscher, C.H. (2017). Mechanical and microstructural properties of metakaolin-based geopolymer cements from sodium waterglass and phosphoric acid solution as hardeners: A comparative study. Applied Clay Science, 140, 81-87.